

Polymorphism in $M(\text{H}_2\text{PO}_2)_3$ ($M = \text{V}, \text{Al}, \text{Ga}$) compounds with the perovskite-related ReO_3 structure.

Hayden A. Evans,^{ab‡} Zeyu Deng,^{cd‡} Ines E. Collings,^e Yue Wu,^c Jessica L. Andrews,^a Kartik Pilar,^b Joshua M. Tuffnell,^f Guang Wu,^a John Wang,^c Siân E. Dutton,^f Paul D. Bristowe,^d Ram Seshadri,^{abg} and Anthony K. Cheetham,^{bcd}

Trivalent metal hypophosphites with the general formula $M(\text{H}_2\text{PO}_2)_3$ ($M = \text{V}, \text{Al}, \text{Ga}$) adopt the ReO_3 structure, with each compound displaying two structural polymorphs. High-pressure synchrotron X-ray studies reveal a pressure-driven phase transition in $\text{Ga}(\text{H}_2\text{PO}_2)_3$ that can be understood on the basis of *ab initio* thermodynamics.

The AMX_3 perovskite structure — well known for accommodating a wide range of chemical substitution — has engendered many interesting compounds and countless avenues of material research. The versatility of the perovskite structure arises from the flexibility to substitute on any of the three chemical sites, A, M, or X, with the tolerance factor serving as a proxy for stability.^{1,2} Over the past decade, there has been considerable focus on hybrid (organic-inorganic) halide perovskites which show great promise in optoelectronic technologies,^{3–6} as well as the related class of alkylammonium metal(II) formates $(\text{A})\text{Mn}^{\text{II}}(\text{HCO}_2)_3$ ⁷ which can display ferroelectric and multiferroic behaviour.^{8,9} Hypophosphite perovskites $\text{AM}(\text{H}_2\text{PO}_2)_3$ compounds are also known.^{10,11}

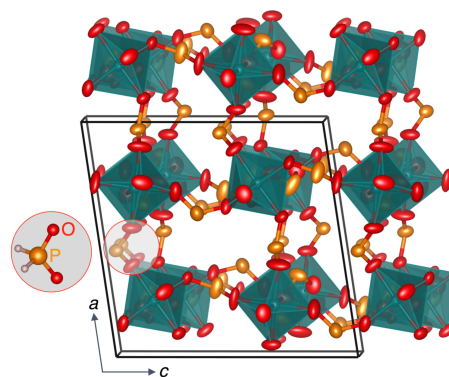


Fig. 1 Representative crystal structure with the ReO_3 topology of α - $M(\text{H}_2\text{PO}_2)_3$, shown for $M = \text{Ga}$ in the $P2_1/n$ space group (90% ellipsoids, H removed for clarity). The inset displays the complete hypophosphite H_2PO_2^- anion.

While not as numerous, there have also been parallel discoveries of ReO_3 -type materials. These compounds are A site deficient: $\square\text{MX}_3$, where \square is a vacancy. MX_3 compounds can vary in X site composition, very much in the manner of AMX_3 perovskites. Besides the oxide (ReO_3),¹² this class includes fluorides,¹³ nitrides,¹⁴ and examples with molecular anions.^{15,16} Some recently reported molecular-anion containing compounds include $\text{Ln}(\text{BH}_4)_3$,¹⁷ $\text{Ln}[\text{C}(\text{NH})_2(\text{NH})]_3$,¹⁸ $\text{In}(\text{imidazolate})_3$,¹⁹ and the $M[\text{Bi}(\text{SCN})_6]$ series,²⁰ demonstrating the impressive richness of X site composition of MX_3 compounds. Since ReO_3 structure materials are known for interesting conductive,^{17,21} structural,^{22,23} barocaloric,²⁴ and optical properties,^{20,25} the ability to control composition is promising from the materials design viewpoint.

In a recent report on the new family of $\text{AMn}^{2+}(\text{H}_2\text{PO}_2)_3$ perovskites made by some of us,¹⁰ it was noted that only one ReO_3 -type $M(\text{H}_2\text{PO}_2)_3$ compound, $\text{V}^{3+}(\text{H}_2\text{PO}_2)_3$, has been documented to date.²⁶ We refer to this compound as α - $\text{V}(\text{H}_2\text{PO}_2)_3$ and employ Greek letters throughout this work to denote unique ReO_3 -

[‡] These authors contributed equally to this work.

^aDepartment of Chemistry and Biochemistry, University of California Santa Barbara, California 93106 United States.

^bMaterials Research Laboratory, University of California Santa Barbara, California 93106 United States. E-mail: akc30@cam.ac.uk

^cDepartment of Materials Science and Engineering, National University of Singapore Singapore 117575, Singapore

^dDepartment of Materials Science and Metallurgy, University of Cambridge 27 Charles Babbage Rd, CB3 0FS Cambridge, UK

^eEuropean Synchrotron Radiation Facility 71 avenue des Martyrs, 38000 Grenoble, France

^fCavendish Laboratory, Department of Physics, University of Cambridge JJ Thomson Avenue, Cambridge CB3 0HE, United Kingdom

^gMaterials Department, University of California Santa Barbara, California 93106 United States

† Electronic Supplementary Information (ESI) available. This includes experimental details, crystallographic files (CCDC 1888648 – 1888652), PXRD, NMR, TGA, and additional DFT calculations. See DOI: 10.1039/b000000x/

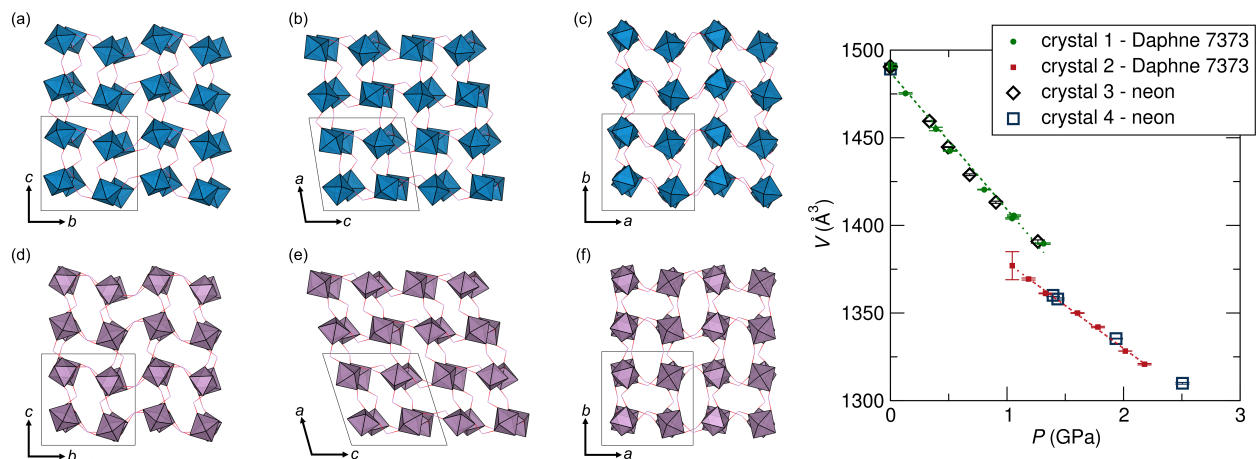


Fig. 2 Pressure-induced phase transition of α -Ga(H₂PO₂)₃. (a,b,c) Views of the ambient pressure crystal structure ($P2_1/n$, $\beta=98.55^\circ$) along the a , b , and c axes. (d,e,f) Views of the high pressure crystal structure ($P2_1/n$, $\beta=107.68^\circ$) along the a , b , and c axes. The graph depicts the cell volumes as a function of pressure of four crystals tested using two different pressure transmitting mediums; Daphne 7373 oil and neon gas. The volume drop upon the phase transition can be observed between ≈ 1.2 GPa and 1.40 GPa. Each crystal was examined over certain ranges to mitigate radiation damage. The ranges for the Daphne oil crystals were 0 GPa – 1.3 GPa, and 1.0 GPa to 2.2 GPa, and for the neon crystals 0 GPa – 1.3 GPa, and 0, 1.4 GPa – 4.8 GPa. The Daphne 7373 oil crystal data was fit with a second order Birch-Murnaghan equation of state (dashed lines).

type polymorphs. In the initial report of α -V(H₂PO₂)₃, the connection with ReO₃ was not noted, and the structure was simply described as 3D connected, with each V atom octahedrally coordinated with H₂PO₂⁻ anions. Inspired by the general interest in ReO₃ type materials, we believed that other related compounds could be made. We report here the successful preparation of a new family of M (H₂PO₂)₃ compounds, where $M = V, Al,$ and $Ga,$ (representative structure displayed in Figure 1), and describe the intriguing polymorphism that each member displays. We also study one of the compounds, α -Ga(H₂PO₂)₃, as a function of hydrostatic pressure, finding a hysteretic first-order phase transition close to a pressure of 1 GPa. We complement the structural work with detailed density functional theory (DFT)-based thermodynamic examination of the P - T phase diagrams of the three systems.

In the original study of α -V(H₂PO₂)₃, crystals of α -V(H₂PO₂)₃ were isolated from a solvothermal reaction between V₂O₃, H₃PO₂, and Li₂(CO₃), and the structure was solved using single crystal X-ray diffraction (SCXRD).²⁶ Based on powder X-ray diffraction (PXRD) of the bulk product, α -V(H₂PO₂)₃ was then established as a minor product alongside an undetermined major phase. Per our subsequent modification of the reported procedure, we successfully isolated crystals of a second polymorph, β -V(H₂PO₂)₃, and Rietveld analysis of the bulk product suggests that this is the unidentified major phase.[†] The β phase ($P2_1/c$) is distinct from the α phase ($P2_1/n$), presenting a less distorted ReO₃ framework. Unlike single atom anion perovskites (e.g. oxides), which display predictable in-phase or out-of-phase octahedral tilt and rotation patterns, molecular anions induce octahedral tilts, rotations, and shifts that are quite complex owing to the greater degrees of freedom. As such, expanded Glazer notation can be used to better describe these systems, and this analysis is presented in the ESI for the phases described in this work.^{†11,27,28}

For the remaining M (H₂PO₂)₃ family members, the metals Al and Ga were chosen as likely M site candidates because of their preferred 3+ oxidation states and similar ionic radii to V³⁺: 0.640 Å, 0.535 Å, and 0.620 Å, respectively for octahedral V³⁺, Al³⁺, and Ga³⁺. It was found that the Al system has two preferred phases: α -Al(H₂PO₂)₃, and a new γ -Al(H₂PO₂)₃ phase. Both polymorphs are obtained together using a solvothermal reaction between H₃PO₂ and Al(O-*i*-Pr)₃, producing α -Al(H₂PO₂)₃ as approximately 10% of the final product, per Rietveld analysis.[†] Although we were unable to make phase-pure α -Al(H₂PO₂)₃, we successfully prepared phase pure γ -Al(H₂PO₂)₃ by substituting γ -Al₂O₃ for Al(O-*i*-Pr)₃ in the solvothermal reaction. The γ phase polymorph crystallizes in the space group $C2/c$ and like the β phase, presents a less distorted structure when compared to the α phase. Interestingly, we have found that while the structure of Al(H₂PO₂)₃ has not been reported, this composition has generated a substantial amount of interest as a flame retardant. When aluminum hypophosphite is added to a polymer blend, there is evidence that the anion reduces the mass transfer pathway, increasing thermal stability,²⁹ in addition to, in some cases, altering the degradation mechanism.³⁰

In all of the synthesis attempts, the Ga system only yielded α -Ga(H₂PO₂)₃ with high phase purity crystal quality. Consequently, high pressure SCXRD experiments were carried out at the European Synchrotron Radiation Facility (ESRF). We hypothesized that under pressure α -Ga(H₂PO₂)₃ may transform to one of the aforementioned, less distorted and consequently denser, polymorphs (β or γ phases). Figure 2 displays views of the structure of α -Ga(H₂PO₂)₃ below and above its pressure-induced phase transition, as well as a plot of T vs. P from the SCXRD refinements at each pressure. As is quite evident, α -Ga(H₂PO₂)₃ undergoes a first-order phase transition near 1.0 GPa to another phase, which is neither β or γ . Instead, α -Ga(H₂PO₂)₃ undergoes a classical isomorphous phase transition to a phase with the same connectiv-

Table 1 Polymorphs seen in all members of the $M(\text{H}_2\text{PO}_2)_3$ family. The columns of each polymorph indicate if/how that phase presents in each metal system. The largest possible pore diameter (\AA) is included in parenthesis.

	α ($P2_1/n$) minor (1.05)	β ($P2_1/c$) major (0.87)	γ ($C2/c$) -	δ ($P2_1/n$) -
V	minor (1.05)	major (0.87)	-	-
Al	minor (0.96)	-	major (0.61)	-
Ga	sole (0.95)	-	-	high pressure (0.71)

ity and space group $P2_1/n$, but with an increased crystallographic β angle of 107.68° (instead of 98.55°). We refer to this high-pressure phase as the δ phase. Upon releasing of this pressure, the α phase is recovered. The bulk modulus of the α phase obtained from the X-ray data is 14.3 GPa, which is substantially lower than the corresponding value for the denser, high pressure δ -phase (27.0 GPa).[†] This is typical behavior for open-to-dense phase transitions under pressure.

In total, we have observed four polymorphs between all M variants studied, with each metal system displaying two polymorphs. Table 1 summarizes these polymorphs, and specifies whether they are the minor, major, sole, or high pressure phases. Crystallographic details of each polymorph can be found in the ESI.[†] It should be noted that the α phase is a shared polymorph between all metal systems at ambient temperature and pressure. However, each system shows distinct behavior, with the Ga system found solely as the α phase under ambient conditions, whereas for Al and V, the α phase occurs only as a minor phase. Considering what would appear to be subtle differences between the α , β , γ , and δ phases, it is curious that certain polymorphs are seen in some metal systems, and not in others. We shed light on this question through DFT calculations by comparing the stability within each systems of the two preferred polymorphs as P and T are varied. The free energy as a function of P and T was calculated by combining DFT and lattice dynamics calculations, as described previously for perovskite formates.³¹ Figure 3 displays the results from the free energy calculations for the three metal systems, with the results further discussed below. We also provide additional details of the thermodynamic analysis in the ESI.[†]

Figure 3(a) shows the stability of the two observed polymorphs for the V system (α and β) as T and P are varied. It can be seen that at ambient temperature and pressure, that the β phase is the preferred polymorph, which is consistent with what is observed experimentally. We had great difficulty synthetically isolating the α phase in our experiments following the reported procedure, and based on Rietveld analysis, it appeared that the only phase observed was the β phase. However, to grow suitable crystals of either phase, we found that the inclusion of Li_2CO_3 was essential (as in the previous report), which could also explain how the α phase may form as a metastable product. Figure 3(b) shows the stability of the two observed polymorphs for the Al system (α and γ). From these calculations our observation of more than one Al polymorph is not surprising, as the calculations suggest that both

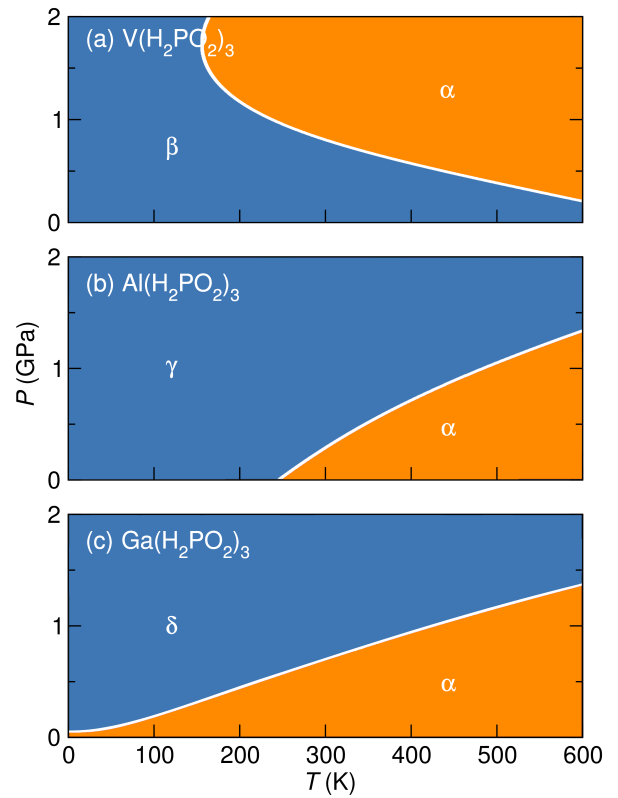


Fig. 3 Calculated P - T phase diagrams for each metal system, and the two observed polymorphs seen each in each. (a) V system, α - β polymorphs. (b) Al system, α - γ polymorphs. (c) Ga system, α - δ polymorphs.

polymorphs are expected to be stable at around ambient T and P . However, due to our success with isolating the γ phase pure by using $\gamma\text{-Al}_2\text{O}_3$, it is feasible that there may well be a synthetic strategy to isolating the α phase pure if the right conditions can be met. Figure 3(c) shows the stability of the two observed polymorphs for the Ga system (α and δ). These calculations predict that the α phase is the preferred phase at ambient pressure and all temperatures, and the δ phase will only form under pressure. This was confirmed experimentally via low temperature PXRD experiments, where no phase transition was observed between 300 K and 12 K.[†] The stability of the α phase down to very low temperatures arises due to its lower zero-point energy relative to the δ phase (Table S8).[†]

It is interesting to note that the α phase is not only common to all three systems, but is also the high temperature phase in each case. The calculations illustrate this by indicating that the α phases have higher entropies compared to the low temperature/high pressure phases.[†] One can regard the high temperature and low temperature phases as open and closed pore systems, respectively, in a manner that is qualitatively similar to certain metal-organic frameworks, such as ZIF-4³² and MIL-53.³³ In particular, larger pores are well known to give rise to enhanced vibrational entropies. The greater pore radii in the α -phases are tabulated in Table 1. The magnitudes of the free volume effects are much smaller than those that have been seen in the metal-organic frameworks (MOFs), but the thermodynamic consequences are

similar.

An issue around the formation of the $M(\text{H}_2\text{PO}_2)_3$ polymorphs is the potential for additional effects due to hydrogen bonding. Surprisingly, there appears to be weak $\text{P-H}\cdots\text{O}$ hydrogen bonding in the α phase, across the faces of the open cavities. In the more dense polymorphs, like the $\gamma\text{-Al}(\text{H}_2\text{PO}_2)_3$ or the high pressure $\delta\text{-Ga}(\text{H}_2\text{PO}_2)_3$ phase, hydrogen bonding does not appear to be present on inspection of the $\text{P-H}\cdots\text{O}$ distances. This is an interesting effect and appears analogous to other perovskite-related systems which display void space due to the effects of hydrogen bonding forces.³⁴ Finally, it is informative to compare this ReO_3 -type hypophosphite family with a closely related family of formate MX_3 compounds. Although the hypophosphites are made absent of any observable moiety within the cavities, the formate family is only isolable when made in the presence of CO_2 , which then resides within the cavities and stabilizes the material.³⁵ For the hypophosphite system this is not the case, as the pore size (diameter of less than 2 \AA) is too small as a consequence of the extra H atoms. This was further confirmed in pressure experiments with neon as a pressure-transmitting medium, where no neon (atomic diameter of 2.4 \AA)³⁶ was found to enter the cavities of the $\text{Ga}(\text{H}_2\text{PO}_2)_3$ structure.

In conclusion, we present a new family of $M(\text{H}_2\text{PO}_2)_3$ compounds displaying unusual polymorphism. Based on the size of the metal cation, certain polymorphs are favored at ambient pressure and temperature, with one phase being shared throughout. Entropic stabilization appears to play an important role in stabilizing the structures.

Conflicts of interest

There are no conflicts to declare.

Acknowledgments

This work was supported by the U.S. Department of Energy, Office of Science, Basic Energy Sciences under award number DE-SC-0012541. The use of the Shared Experimental Facilities of the Materials Research Science and Engineering Center (MRSEC) at UCSB is gratefully acknowledged (NSF DMR 1720256). We acknowledge the provision of beamtime at the European Synchrotron Radiation Facility on the ID15B beamline for the high-pressure work. IEC thanks J. Jacobs for the neon gas load. Calculations were performed using the Cambridge HPCS and the UK National Supercomputing Service, ARCHER. Access to the latter was obtained via the UKCP consortium and funded by EPSRC under Grant No. EP/P022596/1. AKC thanks the Ras al Khaimah Centre for Advanced Materials for financial support.

Notes and references

- 1 V. M. Goldschmidt, *Naturwissenschaften*, 1926, **14**, 477–485.
- 2 G. Kieslich, S. Sun and A. K. Cheetham, *Chem. Sci.*, 2014, **5**, 4712–4715.
- 3 A. Kojima, K. Teshima, Y. Shirai and T. Miyasaka, *J. Am. Chem. Soc.*, 2009, **131**, 6050–6051.
- 4 C. C. Stoumpos and M. G. Kanatzidis, *Acc. Chem. Res.*, 2015, 150909082443006.
- 5 D. H. Fabini, J. G. Labram, A. J. Lehner, J. S. Bechtel, H. A. Evans, A. Van der Ven, F. Wudl, M. L. Chabinyk and R. Seshadri, *Inorg. Chem.*, 2016, **56**, 11–25.
- 6 B. Saparov and D. B. Mitzi, *Chem. Rev.*, 2016, **116**, 4558–4596.
- 7 X.-Y. Wang, L. Gan, S.-W. Zhang and S. Gao, *Inorg. Chem.*, 2004, **43**, 4615–4625.
- 8 P. Jain, N. S. Dalal, B. H. Toby, H. W. Kroto and A. K. Cheetham, *J. Am. Chem. Soc.*, 2008, **130**, 10450–10451.
- 9 P. Jain, V. Ramachandran, R. J. Clark, H. D. Zhou, B. H. Toby, N. S. Dalal, H. W. Kroto and A. K. Cheetham, *J. Am. Chem. Soc.*, 2009, **131**, 13625–13627.
- 10 Y. Wu, S. Shaker, F. Brivio, R. Murugavel, P. D. Bristowe and A. K. Cheetham, *J. Am. Chem. Soc.*, 2017, **139**, 16999–17002.
- 11 Y. Wu, T. Binford, J. A. Hill, S. Shaker, J. Wang and A. K. Cheetham, *Chemical Commun.*, 2018, **54**, 3751–3754.
- 12 D. V. S. Muthu, P. Teredesai, S. Saha, U. V. Waghmare, A. K. Sood and C. N. R. Rao, *Phys. Rev. B*, 2015, **91**, 224308.
- 13 B. K. Greve, K. L. Martin, P. L. Lee, P. J. Chupas, K. W. Chapman and A. P. Wilkinson, *J. Am. Chem. Soc.*, 2010, **132**, 15496–15498.
- 14 R. K. Sithole, L. F. E. Machogo, M. A. Airo, S. S. Gqoba, M. J. Moloto, P. Shumbula, J. Van Wyk and N. Moloto, *New J. Chem.*, 2018, **42**, 3042–3049.
- 15 A. A. Karyakin, *Electroanalysis*, 2001, **13**, 813–819.
- 16 S. Ferlay, T. Mallah, R. Ouahes, P. Veillet and M. Verdaguier, *Nature*, 1995, **378**, 701.
- 17 M. B. Ley, M. Jørgensen, R. Cerny, Y. Filinchuk and T. R. Jensen, *Inorg. Chem.*, 2016, **55**, 9748–9756.
- 18 A. L. Goörne, J. George, J. van Leusen, G. Dück, P. Jacobs, N. K. Chogondahalli Muniraju and R. Dronskowski, *Inorg. Chem.*, 2016, **55**, 6161–6168.
- 19 M. E. Schweinefuß, I. A. Baburin, C. A. Schröder, C. Näther, S. Leoni and M. Wiebcke, *Cryst. Growth Des.*, 2014, **14**, 4664–4673.
- 20 M. J. Cliffe, E. N. Keyzer, M. T. Dunstan, S. Ahmad, M. F. L. De Volder, F. Deschler, A. J. Morris and C. P. Grey, *Chem. Sci.*, 2019, **42**, 3042–3049.
- 21 A. Ferretti, D. B. Rogers and J. B. Goodenough, *J. Phys. Chem. Solids*, 1965, **26**, 2007–2011.
- 22 J. O. Ticknor, B. R. Hester, J. W. Adkins, W. Xu, A. A. Yakovenko and A. P. Wilkinson, *Chem. Mater.*, 2018, **30**, 3071–3077.
- 23 C. Yang, P. Tong, J. C. Lin, X. G. Guo, K. Zhang, M. Wang, Y. Wu, S. Lin, P. C. Huang and W. Xu, *Appl. Phys. Lett.*, 2016, **109**, 23110.
- 24 A. Corrales-Salazar, R. T. Brierley, P. B. Littlewood and G. G. Guzmán-Verri, *Phys. Rev. Mater.*, 2017, **1**, 53601.
- 25 C. G. Granqvist, *Appl. Phys. A*, 1993, **57**, 3–12.
- 26 H. A. Maouel, V. Alonzo, T. Roisnel, H. Rebbah and E. Le Fur, *Acta Crystallogr. C*, 2009, **65**, i36–i38.
- 27 J. A. Hill, A. L. Thompson and A. L. Goodwin, *J. Am. Chem. Soc.*, 2016, **138**, 5886–5896.
- 28 H. L. B. Boström, J. A. Hill and A. L. Goodwin, *Phys. Chem. Chem. Phys.*, 2016, **18**, 31881–31894.
- 29 W. Yang, Z. Jia, Y. Chen, Y. Zhang, J. Si, H. Lu and B. Yang, *RSC Adv.*, 2015, **5**, 105869–105879.
- 30 B. Zhao, L. Chen, J.-W. Long, H.-B. Chen and Y.-Z. Wang, *Ind. Eng. Chem. Res.*, 2013, **52**, 2875–2886.
- 31 G. Kieslich, S. Kumagai, K. T. Butler, T. Okamura, C. H. Hendon, S. Sun, M. Yamashita, A. Walsh and A. K. Cheetham, *Chem. Commun.*, 2015, **51**, 15538–15541.
- 32 M. T. Wharmby, S. Henke, T. D. Bennett, S. R. Bajpe, I. Schwedler, S. P. Thompson, F. Gozzo, P. Simoncic, C. Mellot-Draznieks, H. Tao, Y. Yue and A. K. Cheetham, *Angew. Chem. Int. Ed.*, 2015, **54**, 6447–6451.
- 33 A. Boutin, F.-X. Coudert, M.-A. Springuel-Huet, A. V. Neimark, G. Férey and A. H. Fuchs, *J. Phys. Chem. C*, 2010, **114**, 22237–22244.
- 34 H. A. Evans, D. H. Fabini, J. L. Andrews, M. Koerner, M. B. Preefer, G. Wu, F. Wudl, A. K. Cheetham and R. Seshadri, *Inorg. Chem.*, 2018, **57**, 10375–10382.
- 35 Y.-Q. Tian, Y.-M. Zhao, H.-J. Xu and C.-Y. Chi, *Inorg. Chem.*, 2007, **46**, 1612–1616.
- 36 J. K. Badenhoop and F. Weinhold, *J. Chem. Phys.*, 1997, **107**, 5422–5432.